8 Niue

© Molly Brown, NZ

8.1 Summary

8.1.1 Climate

- Changes in air temperature from season to season are relatively small and strongly linked to changes in the surrounding ocean temperature. Niue has two distinct seasons – a warm wet season from November to April and a cooler dry season from May to October.
- The seasonal cycle is strongly affected by the South Pacific Convergence Zone (SPCZ), which is most intense during the wet season.
- Annual and seasonal air temperatures at Alofi–Hanan Airport increased over the period 1951–2020.
- Annual and seasonal rainfall trends, as well as trends in rainfall extremes, show little change at Alofi–Hanan Airport.
- Tropical cyclones usually affect Niue between November and April. Over the period 1969–2018, an average of 16 cyclones passed within the Niue exclusive economic zone (EEZ) per decade. Tropical cyclones were most frequent in neutral or El Niño years and least frequent in La Niña years. Year-to-year variability is large, ranging from no tropical cyclones in some seasons to four.
- There has been little change in the total number of tropical cyclones in the Southwest Pacific since 1981/82. The number of severe tropical cyclones has declined over the same period/region.

8.1.2 Ocean

- Highest sea levels typically occur in the months November–February.
- Sea-level rise within the EEZ, measured by satellite altimeters since 1993, is about 3 to 5 mm per year.
- Monthly average ocean temperature, as measured by the Niue tide-gauge, ranges from 25.2 °C in August to 28.2 °C in March. However, monthly temperatures in any given year can be up to ±2 °C of these averages.
- The sea surface temperature (SST) trend, as per satellite observations, is 0.29 °C per decade, one of the highest trends in the Southwest Pacific.
- Dominant wave direction is from 212° (SSW), with an average significant wave height of 1.73 m and average wave period of 13.48 s.
- Severe wave height was defined as 3.65 m, with an average of 3.1 severe events per year.
- Peak average significant wave height occurs around July.

8.2 Country description

Niue is an island country located in the tropical western South Pacific Ocean between latitudes 18.5°S and 19.5°S, and longitudes 169°W and 170°W. It has a total land area of 261 km^2 and an EEZ of 127,000 km^2. Alofi, the capital is located on the west coast. The highest elevation is 68 m above sea level. Niue's population is approximately 1600.

Figure 8.1:
Niue and the location of the climate station used in this report

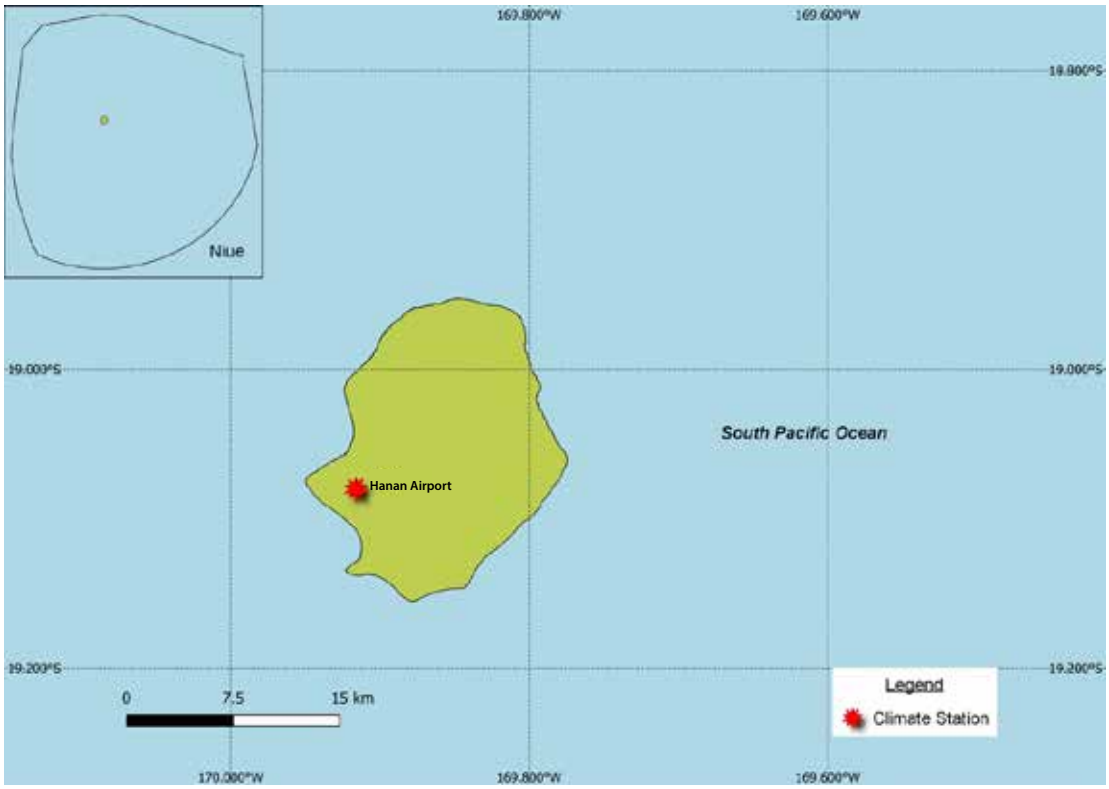

8.3 Data

Daily historical rainfall and air temperature records for an Alofi–Hanan Airport (Hanan Airport hereafter) station composite from 1951 were obtained from the Niue Meteorological Service. These records have undergone data quality and homogeneity assessment. Where the maximum or minimum air temperature records were found to have discontinuities, these records have been adjusted to make them homogeneous (further information is provided in Chapter 1). Additional information on historical climate trends for Niue can be found in the Pacific Climate Change Data Portal http://www.bom.gov.au/climate/pccsp.

Tropical cyclone data and historical tracks starting from the 1969/70 season are available from the SHTC Data Portal http://www.bom.gov.au/cyclone/history/tracks/index.shtml.

SST covering the EEZ was obtained via the daily Optimum Interpolation SST version 2.1 (OISST v2.1) dataset from NOAA (Reynolds et al. 2007; Banzon et al. 2016). In situ ocean temperature data were obtained from the PSLGM Project tide-gauge located at Alofi, with data spanning from 2015 to 2019.

Wave data were obtained from the PACCSAP wave hindcast (Smith et al. 2021), available hourly from 1979 to present, with a grid resolution near Niue of 7 km.

Regional sea level data were obtained from CSIRO satellite altimetry (updated by Benoit Legresy, Church and White 2011), with correction for seasonal signals, inverse barometer effect and glacial isostatic adjustment. Tide-gauge data were sourced from the Alofi tide-gauge station, spanning from 1993 to 2021 at hourly intervals.

8.4 Rainfall

8.4.1 Seasonal cycle

During the wetter/warmer half of the year from November to April, the trade winds weaken and the SPCZ is most active, leading to almost two thirds of Hanan Airport's rain to fall during this period (Figure 8.2). This reflects the importance of the SPCZ on rainfall, which is most active during the wet season months and positioned closest to Niue, compared to the dry season where the SPCZ is further to the northeast and less active.

Niue's climate is also influenced by subtropical high-pressure systems and the trade winds, which blow mainly from the southeast.

Figure 8.2:
Mean annual rainfall at Hanan Airport

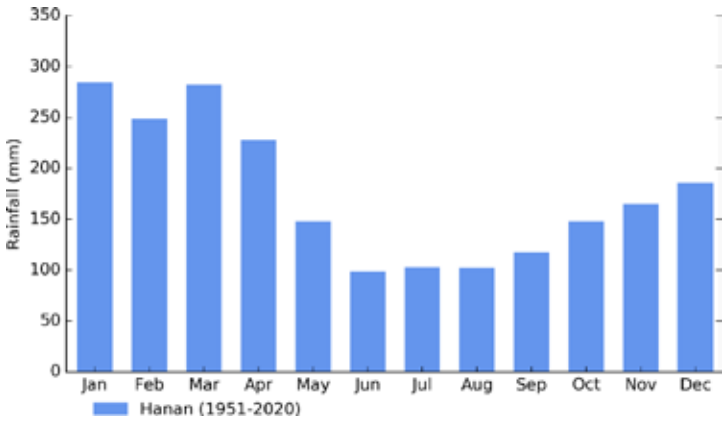

8.4.2 Trends

Trends in annual and seasonal rainfall since 1951 are not statistically significant at Hanan Airport (Figure 8.3, Table 8.1). Annual and seasonal rainfall trends indicate little change. Variability associated with El Niño–Southern Oscillation (ENSO) is evident, with La Niña years generally experiencing higher rainfall than El Niño years. Annual rainfall at Hanan Airport varies from approximately 800 to 3900 mm.

Figure 8.3:
Annual rainfall (bar graph) and number of wet days (where rainfall is at least 1 mm; line graph) at Hanan Airport. Straight lines indicate linear trends for annual rainfall (in black) and number of wet days (in blue). The magnitudes of the trends are presented in Table 8.1.

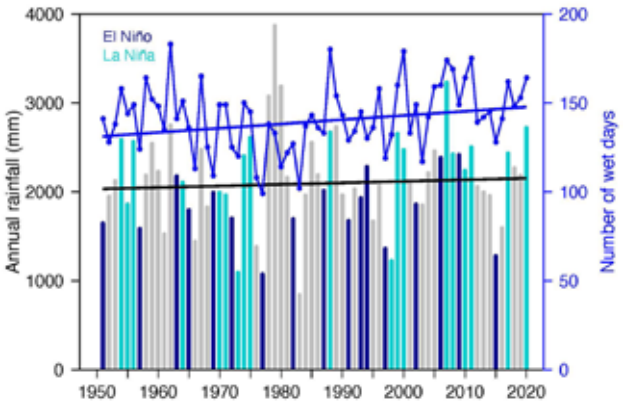

Table 8.1:
Trends in annual, seasonal and extreme rainfall at Hanan Airport. The 95% confidence intervals are shown in parentheses. The contribution to total rainfall from extreme events and the standardised rainfall evapotranspiration index are measured relative to 1961–1990 (see Chapter 1 for details).

	Hanan Airport
	1951–2020
Annual rainfall (mm/decade)	+17.09 (-63.13, +101.24)
November–April (mm/decade)	+5.18 (-46.02, +50.09)
May–October (mm/decade)	+19.60 (-22.56, +60.44)
Number of wet days (days/decade)	+2.39 (-0.40, +5.27)
Contribution to total rainfall from extreme events (%/decade)	-0.41 (-1.73, +0.92)
Consecutive dry days (days/decade)	0.00 (-0.49, +0.41)
Maximum one-day rainfall (mm/decade)	-0.21 (-5.60, +5.52)
Standardised rainfall evapotranspiration index (November–April)	-0.01 (-0.12, +0.09)
Standardised rainfall evapotranspiration index (May–October)	+0.06 (-0.04, +0.17)

Similar to annual and seasonal rainfall, no significant trends in extreme rainfall indices, including the standardised rainfall evapotranspiration drought index, were detected (Table 8.1). Figure 8.4 shows low interannual variability in consecutive dry days and most years do not experience more than three weeks without rain.

Figure 8.4:
Annual longest run of consecutive dry days (bar graph) and maximum daily rainfall (line graph) at Hanan Airport. Straight lines indicate linear trends for dry days (in black) and maximum daily rainfall (in blue). The magnitudes of the trends are presented in Table 8.1.

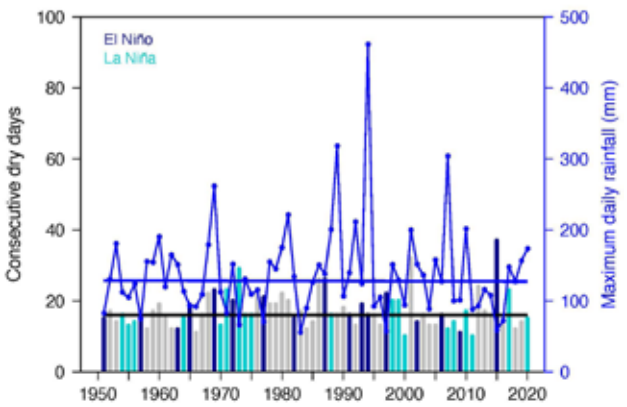

8.5 Air temperature

8.5.1 Seasonal cycle

The range in average monthly maximum and minimum temperatures throughout the year at Hanan Airport is 4 ºC for the 1961–1990 climatology period and 3.7 ºC for the 1991–2020 period. There has been a clear shift towards warmer average monthly temperatures between the climatology periods of 1961–1990 and 1991–2020 (Figure 8.5), with warmer average temperatures occurring in all months throughout the year, with the exception of May average minimum temperatures. The largest increase in average minimum temperatures occurs during July and August, with almost 1 ºC of warming, while average maximum temperatures have seen the largest warming between July and December.

Figure 8.5:
Maximum and minimum air temperature seasonal cycle for Hanan Airport for the periods 1961–1990 (dotted lines) and 1991–2020 (solid lines)

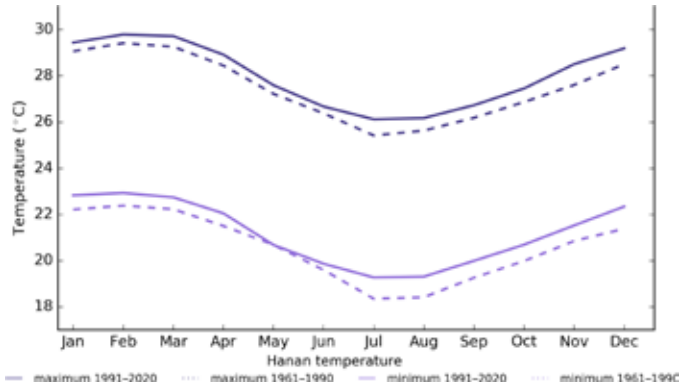

8.5.2 Trends

Average annual and seasonal temperatures have increased significantly at Hanan Airport (Figure 8.6). November–April temperatures are warming at approximately the same rate as May–October temperatures (Table 8.2).

Figure 8.6:
Average annual, November–April and May–October temperatures for Hanan Airport. Straight lines indicate linear trends. The magnitudes of the trends are presented in Table 8.2. Diamonds indicate years with insufficient data for one or more variables.

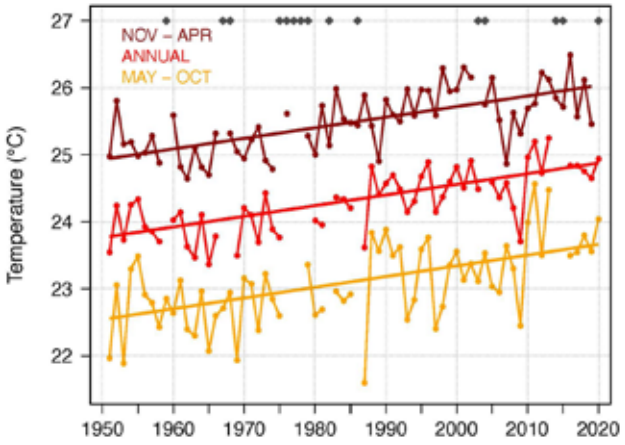

Table 8.2:
Trends in annual and seasonal air temperatures at Hanan Airport. The 95% confidence intervals are shown in parentheses, and trends significant at the 95% level are shown in bold.

	Hanan Airport Tmax (°C/decade)	Hanan Airport Tmin (°C/decade)	Hanan Airport Tmean (°C/decade)
	1951–2020		
Annual	**+0.16** (+0.12, +0.21)	**+0.15** (+0.09, +0.2)	**+0.16** (+0.11, +0.21)
November–April	**+0.19** (+0.13, +0.24)	**+0.13** (+0.05, +0.2)	**+0.16** (+0.11, +0.22)
May–October	**+0.17** (+0.08, +0.24)	**+0.16** (+0.10, +0.23)	**+0.16** (+0.10, +0.23)

Numerous gaps exist in the daily temperature record for Hanan Airport, which prevents the robust calculation of trends for most temperature extremes. However, Figure 8.7 shows that most years since 2010 have experienced over twice as many hot days compared with the beginning of the record. This is consistent with the increases in annual and seasonal temperatures (Figure 8.6) as well as trends in temperature extremes in neighbouring Pacific Island countries.

Figure 8.7:
Annual number of hot days and cold nights at Hanan Airport. The straight line indicates a linear trend for cold nights. Criteria for statistical robustness were not met for determining a linear trend for hot days. Diamonds indicate years with insufficient data for one or both variables.

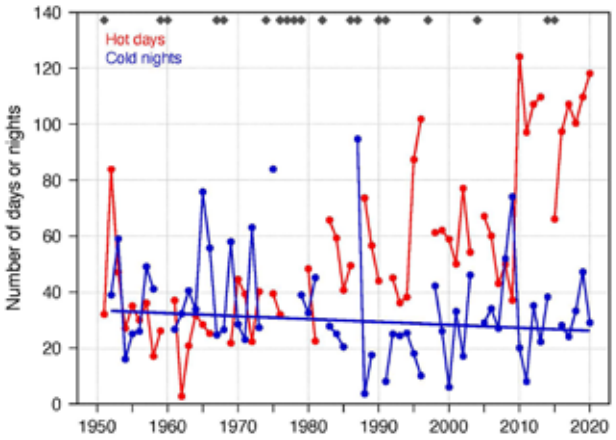

8.6 Tropical cyclones

8.6.1 Seasonal cycle

Tropical cyclones usually affect Niue during the southern hemisphere tropical cyclone season, which is from November to April, but also occasionally occur outside the tropical cyclone season. The Southern Hemisphere Tropical Cyclone Archive indicates that between the 1969/70 and 2017/18 seasons, 51 tropical cyclones (Figure 8.8) passed within the EEZ. This represents an average of 10 cyclones per decade. Tropical cyclones were most frequent in neutral or El Niño years (12 cyclones per decade) and least frequent in La Niña years (7 cyclones per decade).

Interannual variability in the number of tropical cyclones in the EEZ is large, ranging from zero in some seasons to four in 1979/80, 2002/03 and 2015/16 (Figure 8.8). High interannual variability and the small number of tropical cyclones occurring in the EEZ make reliable identification of long-term trends in frequency and intensity difficult.

Some tropical cyclone tracks analysed in this section include the tropical depression stage (sustained winds ≤34 knots) before and/or after tropical cyclone formation.

Figure 8.8:
Number of tropical cyclones passing within the Niue EEZ per season. Each season is defined by the ENSO status, with light blue being an El Niño year, dark blue a La Niña year and grey showing a neutral ENSO year. The 11-year moving average is presented as a purple line and considers all years.

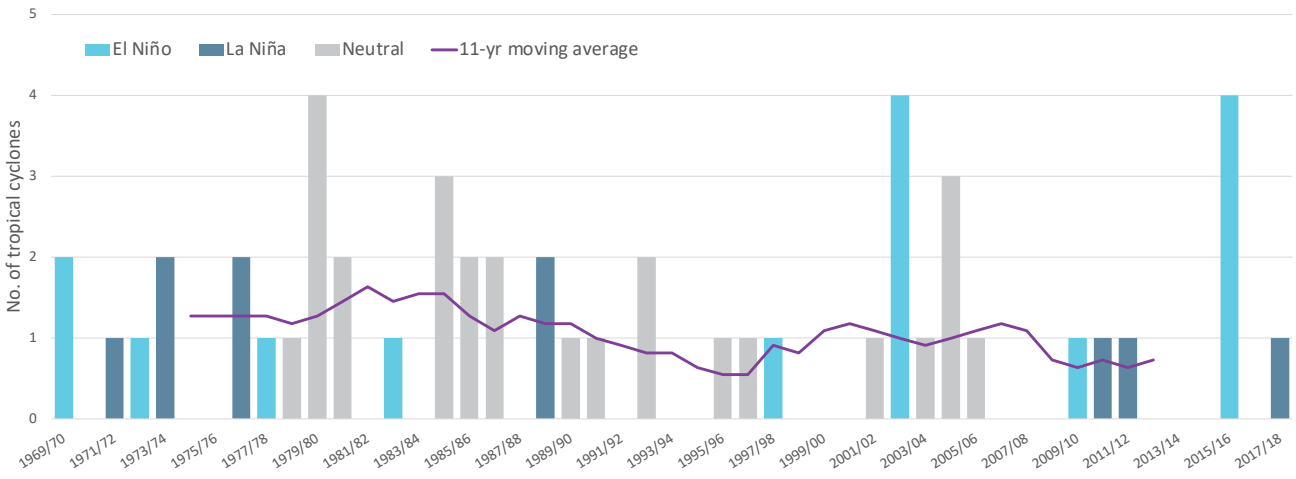

8.6.2 Trends

Trends in total number of tropical cyclones (<995 hPa) and severe tropical cyclones (<970 hPa) are presented for the period 1981/82–2020/21 for the greater Southwest Pacific (135°E–120°W; 0–50°S). Trends are presented at a regional scale as the number of tropical cyclones occurring within Pacific Island EEZs is insufficient for reliable long-term trend analysis.

For the total number of tropical cyclones, the trend (and 95% confidence interval) is -0.92(-1.85, 0.01) tropical cyclones/decade. There has been little change/marginal decline in the total number of tropical cyclones over the last 40 seasons. This trend is not statistically significant.

For the total number of severe tropical cyclones, the trend is -0.80 (-1.32, -0.29) tropical cyclones/decade. There is a negative trend in the number of severe tropical cyclones over the last 40 seasons. There has been little change/marginal decline in the proportion of tropical cyclones reaching severe status. The trend is -0.04 (-0.08, 0.00) tropical cyclones/decade. The negative trend is statistically significant.

Records of tropical cyclones exist from the late 1800s in some countries in the Southwest Pacific, but trends in tropical cyclones have only been presented from 1981/82. Satellite-based observations began in the Southwest Pacific in the early 1970s, but consistent coverage and reliable intensity estimates have only been available since the early 1980s. Confidence in tropical cyclone trends is moderate as the definition of a tropical cyclone has changed and satellite observation methods have continued to improve over the last 40 years.

8.7 Sea surface temperature

8.7.1 Seasonal cycle

Ocean temperature, as measured by the Niue tide-gauge from 2016 to 2019, reaches on average a maximum of 28.2 °C in March, but individual months can get as high as 29.5 °C. Minimum average temperatures reach a low of 25.2 °C in August. Temperatures can be up to 2 °C higher or lower than these averages, although 50% of observations fall within 1.5 °C of the average. This is a very short temperature record, so temperature ranges shown in Figure 8.9 may not fully represent seasonal conditions over decadal timescales.

Figure 8.9:
Annual temperatures measured at the Niue tide-gauge. Blue dots show the monthly average, and shaded boxes show the middle 50% of observations. Lines show the top and bottom 25% of observations.

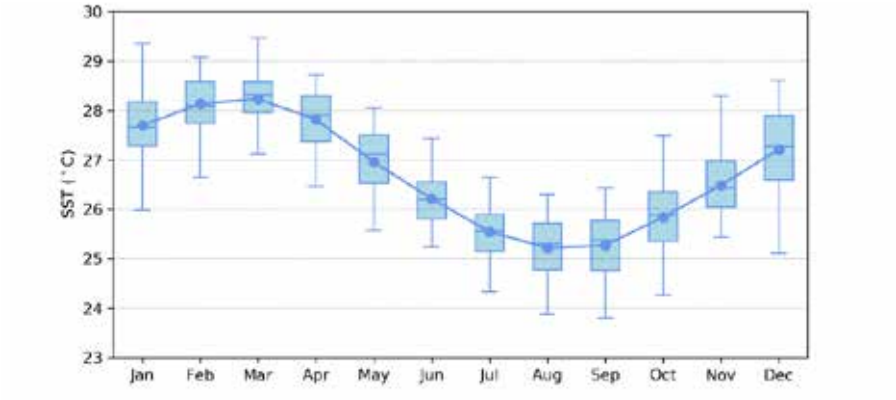

8.7.2 Trends

Figure 8.10 shows the 1981–2021 SST from satellite observations averaged over the Niue EEZ. The data show a trend of 0.29 °C per decade with a 95% confidence interval of ±0.10 °C.

Figure 8.10:
Sea surface temperature from satellite observations averaged across the Niue EEZ, shown as the orange line. The blue line shows the linear regression trend.

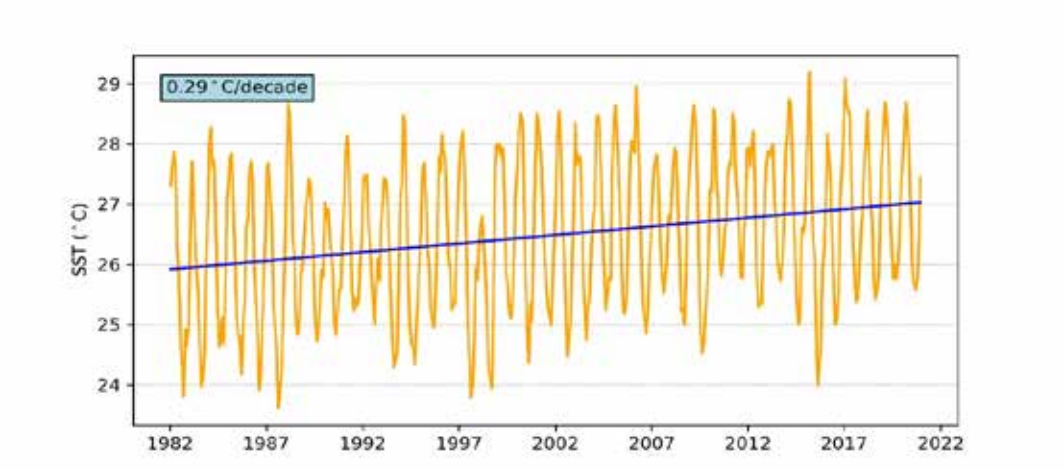

8.8 Sea level

8.8.1 Seasonal cycle

Niue experiences a semidiurnal tidal cycle, meaning two high and two low tides per day. The highest predicted tides of the year typically occur during the wet season months of December to February. Figure 8.11 shows the number of hours the 99th percentile (1.53 m) sea level threshold is exceeded per month across the entire sea level record at Niue. Peak sea levels typically occur in November–February.

Figure 8.11:
Number of hours exceeding 99th percentile sea level threshold per month from 2015 to 2019 at the Niue tide-gauge. Blue shading indicates the number of hours, and the final row provides a percentage summary of all the years.

Number of hours exceeding 1.53 m (Alofi Wharf, Niue)

	Jan	Feb	Mar	Apr	May	Jun	Jul	Aug	Sep	Oct	Nov	Dec	Annual
2015	0	0	0	0	0	0	0	0	0	0	2	0	2
2016	2	0	0	0	0	0	0	0	0	0	0	0	2
2017	0	4	0	0	0	0	0	0	0	0	1	10	15
2018	0	0	0	0	0	0	0	3	0	0	0	0	3
2019	0	4	0	0	0	0	0	0	0	0	0	4	8
Monthly Totals (%)	7	27	0	0	0	0	0	10	0	0	10	47	

8.8.2 Trends

Sea level at Niue, measured by satellite altimeters (Figure 8.12) since 1993, has risen between 3 and 5 mm per year across the EEZ (the highest in the south), with a 95% confidence interval of ±0.4 to ±0.6 mm. This rise is partly linked to a pattern related to climate variability from year to year and decade to decade. Most of the EEZ has a higher sea level trend than the global average of 3.1 ± 0.4 mm per year (von Schuckmann et al. 2021).

Figure 8.12:
Satellite altimetry annual trend for the Pacific from 1993 to 2020, with Niue EEZ highlighted. The star symbol indicates the location of the tide-gauge.

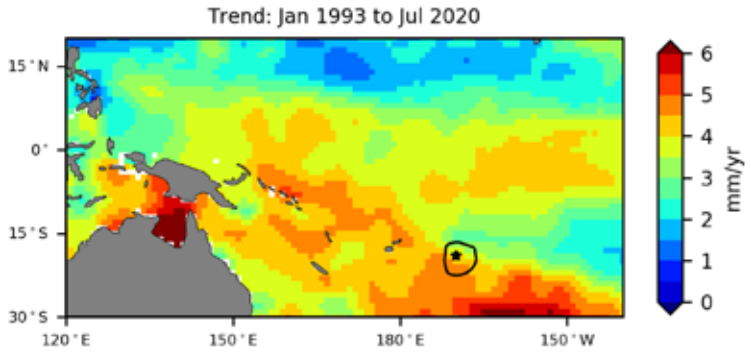

8.9 Waves

8.9.1 Seasonal cycle

The average wave climate in Niue is defined by the significant wave height, peak period and peak direction. The significant wave height is the mean wave height (from trough to crest) of the highest one third of waves and corresponds to the wave height that would be reported by an experienced observer. Peak period is the time interval between two waves of the dominant wave period. Peak direction is the direction from which the dominant waves are coming.

The average sea state is dominated by swells from the south. The annual mean wave height is 1.73 m, the annual mean wave direction is 212° and the annual mean wave period is 13.48 s. In the Pacific, waves often come from multiple directions and for different periods at a time. In Niue, there are often more than four different wave direction/period components coming from the southeast to southwest (Figure 8.13).

Figure 8.13:
Annual wave rose for Niue. Note that direction is where the wave is coming from Seasonal wave height peaks in July, whereas the seasonal wave period peaks in September/October (Figure 8.14). This is related to the intensification of the Southern Ocean storm track during winter (June–August). Conversely, there is slightly reduced wave activity during the summer (December–February) months.

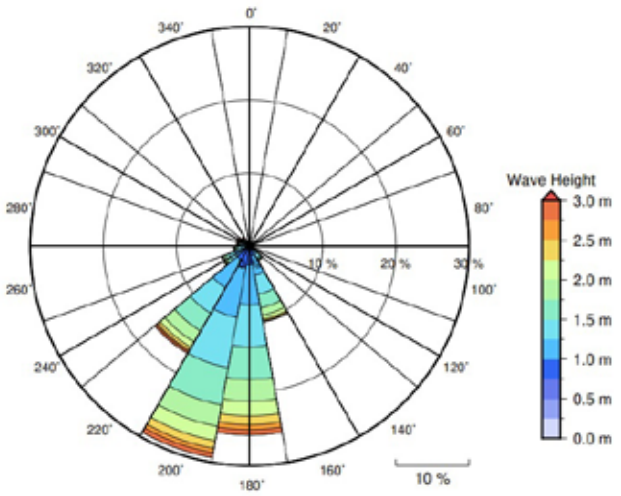

Figure 8.14:
Monthly wave height (black line), wave period (red line) and wave direction (arrows). The grey area represents the range of wave height between calm periods (10% of lowest wave height) and large wave events (10% of highest wave height).

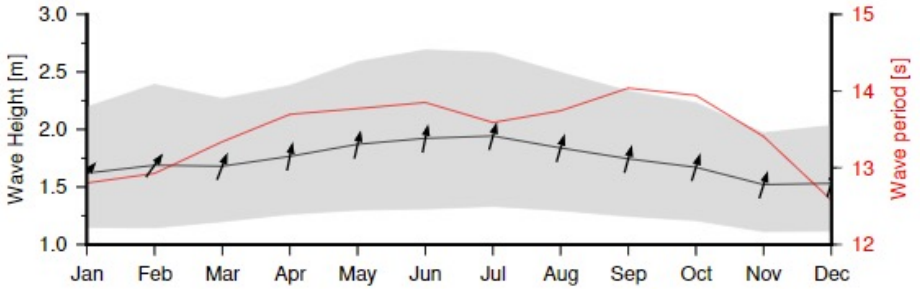

8.9.2 Trends

Waves change from month to month with the seasons, but they also change from year to year with climate oscillations. Typically, these changes are smaller than the seasonal changes but can be important during phenomena such as ENSO. In Niue, the mean annual wave height has remained unchanged since 1979 (Figure 8.15). The mean annual wave height in Niue is not significantly correlated with the main climate indicators of the region.

Figure 8.15:
Annual wave height (black line), wave period (red line) and wave direction (arrows). The grey area represents the range of wave height between calm periods (10% of lowest wave height) and large wave events (10% of highest wave height).

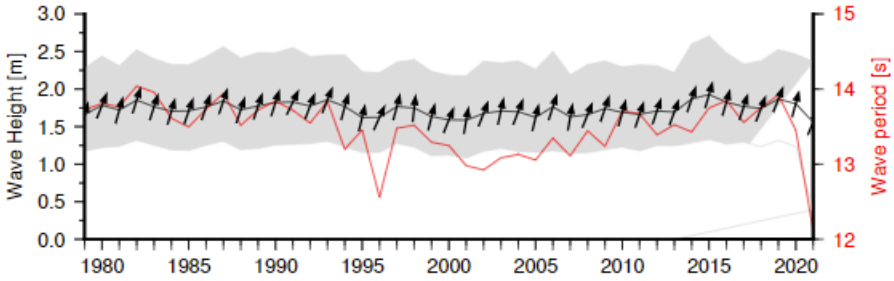

8.9.3 Extreme waves

Extreme wave analysis completed for Niue was done by defining a severe height threshold and fitting a generalized Pareto distribution (GPD). The optimum threshold selected was 3.65 m. In the 42-year wave hindcast, 131 wave events reached or exceeded this threshold, averaging 3.1 per year. The GPD was fitted to the largest wave height reached during each of these events (Figure 8.16, Table 8.4). Extreme wave analysis is a very useful tool but is not always accurate because the analysis is very sensitive to the data available, the type of distribution fitted and the threshold used. For example, this analysis does not accurately account for tropical cyclone waves. More in-depth analysis is required to obtain results appropriate for designing coastal infrastructure and coastal hazard planning.

Figure 8.16:
Extreme wave distribution for Niue. The crosses represent the wave events that have occurred since 1979. The solid line is the statistical distribution that best fits past wave events. The dashed lines show the upper and lower confidence limits of the fit. There is a 95% chance that the fitted distribution lies between the two dashed lines. Note that the annual return interval is in logarithmic scale.

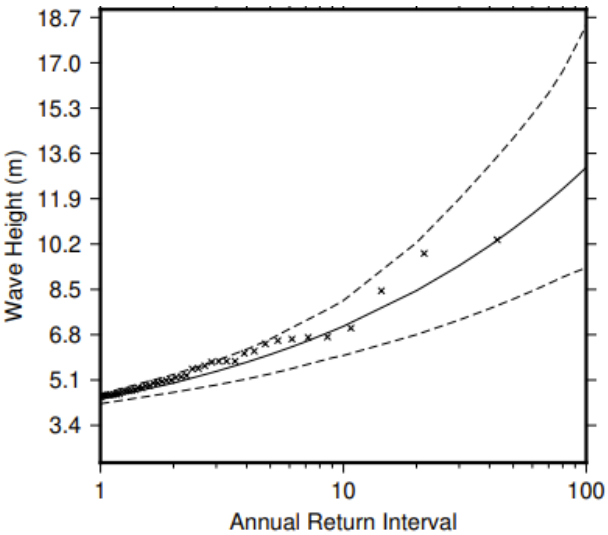

Table 8.4: Summary of the results from extreme wave analysis in Niue

Large wave height (90th percentile)	2.38 m
Severe wave height (99th percentile)	3.41 m
1-year ARI wave height	4.37 m
10-year ARI wave height	7.12 m
20-year ARI wave height	8.45 m
50-year ARI wave height	10.77 m
100-year ARI wave height	13.07 m